Supporting Information

Max et al. 10.1073/pnas.1714397115

SI Text: Method Optimization of exRNA and exDNA Isolation

SI Results. Optimizing exRNA and exDNA isolation was an iterative process that required several rounds of optimization, briefly outlined here looking at four distinct developmental stages (Fig. S1 *A–D*); the details of the experimental conditions are listed in *SI Materials and Methods*. RNA intactness was visualized by phosphorimaging of ^{32}P-labeled spike-in DNA and RNA tracers and their degradation products. The tracers were added with the denaturant solution or organic extraction solution when the biofluid was first contacted.

In Fig. S1*A*, RNA isolated from serum using a commercial RNA organic extraction protocol based on TRIzol LS followed by ethanol precipitation showed notable tracer degradation (lane 1), while degradation did not occur in a water sample (lane 2), suggesting carryover and refolding of RNase trace amounts from the biofluid. Sample preincubation in detergent (2% SDS) or chaotrope (4 M GITC) at 50 °C before organic extraction, demonstrated the best protection in this comparison (lanes 3 and 4).

In Fig. S1*B*, silica-matrix adsorption-based RNA purification, based on the commercial RNeasy MinElute Cleanup Kit (Qiagen) following organic extraction showed greater tracer integrities when using the TRIzol-based protocol (lanes 1 and 2), but also in this setting hot preincubation in denaturants followed by organic extraction improved RNA integrity (lanes 3–6). Under these conditions, small RNAs (19–31 nt) appeared in the flowthrough of TRIzol LS extractions after column purification (lanes 2 and 4), likely due to reduced binding of miRNAs and other fragmented RNAs. While it was possible to decrease losses in this size range by lowering the solvent polarity through increasing alcohol concentrations before column binding, this adjustment favored clogging of spin-columns, likely due to increased precipitation of proteins from the aqueous phase.

In Fig. S1*C*, an addition of proteinase K during sample pretreatment prevented column clogs and allowed using ≥66% isopropanol to improve recovery of small RNAs. More importantly, however, proteinase K pretreatment in SDS eliminated interphase formation after phase separation and enabled automated aspirations of aqueous phases after extraction, which had been the most time-consuming step in the entire procedure.

In Fig. S1*D*, proteinase K treatment in SDS also improved RNA integrity of the longer 45-mer and 500-mer RNA tracers (lane 4), compared with hot incubations with chaotrope (GITC), where enzymatic activity and interphase depletion were reduced, especially after overnight incubation (lane 2), suggesting that residual RNase trace amounts were present. Increasing SDS concentrations to 5.5% and temperatures to 65 °C did not notably affect proteinase K activity, and in combination with added reducing agents, these adjustments helped to eliminate residual RNase activity in biofluid samples, which otherwise showed low tracer RNA integrity. The addition of a reformulated extraction solution following enzymatic digestion at 65 °C enabled using single-phase mixtures of aqueous and organic solutions at a ratio of 1.15:1 (digestion reaction:extraction agent), compared with ratios of 1:3 for TRIzol LS and 1:4 for TRIzol and similar alternatives. This reduction allowed almost doubling of the sample volume (vol) to 450 μL and compliance with recommended biofluid input volumes for exRNA isolation (https://exrna.org/resources/protocols/) without having to split samples into two different tubes when using standard liquid handling equipment, including 1.5- and 2-mL microcentrifuge tubes and 1- and 2-mL 96-well deep-well plates. To avoid rapid evaporation and to favor phase separation, the extractions were cooled to 10 °C before chloroform additions. Finally, discovering that controlling GITC concentrations allowed directing DNA tracers between aqueous and organic phases enabled selective recovery of exDNAs in a separate aqueous fraction following exRNA isolation (Fig. 1*A*).

SI Materials and Methods. This section describes procedures and experimental conditions evaluated and applied for method optimization (Fig. S1). It also lists all synthetic oligonucleotides used in extracellular nucleic acid isolation and sRNA-derived cDNA library preparation.

Oligonucleotides. 2′-*O*-methyl oligoribonucleotides (2′-*O*-meRNA) and 2′ deoxyoligonucleotides (DNA), used as size markers during RNA isolation and cDNA library preparation, were purchased from Integrated DNA Technologies. Oligoribonucleotides (RNA) were purchased from Thermo Fisher (Thermo Fisher Scientific) and synthesized in our laboratory. Preadenylated 3′-adapter deoxyoligonucleotides (n = 24), each containing a unique pentamer barcode sequence at the 5′ end and an amino-modifier at the 3′ end, were ligated to samples as described previously (29). Two different sets of calibrator oligoribonucleotides were used: Set1 allowed to monitor and quantify miRNA isolations from biofluids and Set2 was applied to determine RNA isolation efficiencies and monitor cDNA library preparations. Single-stranded oligonucleotide size markers were 5′ radiolabeled as described previously (29).

List of 3′-adapters (for RNA ligation/cDNA library preparation).

Adapter	Sequence
1	rAppTCACTTCGTATGCCGTCTTCTGCTTG-L
2	rAppTCATCTCGTATGCCGTCTTCTGCTTG-L
3	rAppTCCACTCGTATGCCGTCTTCTGCTTG-L
4	rAppTCCGTTCGTATGCCGTCTTCTGCTTG-L
5	rAppTCCTATCGTATGCCGTCTTCTGCTTG-L
6	rAppTCGATTCGTATGCCGTCTTCTGCTTG-L
7	rAppTCGCGTCGTATGCCGTCTTCTGCTTG-L
8	rAppTCTAGTCGTATGCCGTCTTCTGCTTG-L
9	rAppTCTCCTCGTATGCCGTCTTCTGCTTG-L
10	rAppTTAAGTCGTATGCCGTCTTCTGCTTG-L
11	rAppTAACGTCGTATGCCGTCTTCTGCTTG-L
12	rAppTAATATCGTATGCCGTCTTCTGCTTG-L
13	rAppTAGAGTCGTATGCCGTCTTCTGCTTG-L
14	rAppTATCATCGTATGCCGTCTTCTGCTTG-L
15	rAppTGATGTCGTATGCCGTCTTCTGCTTG-L
16	rAppTTACATCGTATGCCGTCTTCTGCTTG-L
17	rAppTACTCTCGTATGCCGTCTTCTGCTTG-L
18	rAppTAGCCTCGTATGCCGTCTTCTGCTTG-L
19	rAppTTATTTCGTATGCCGTCTTCTGCTTG-L
20	rAppTTCATTCGTATGCCGTCTTCTGCTTG-L
21	rAppTTGACTCGTATGCCGTCTTCTGCTTG-L
22	rAppTTGTATCGTATGCCGTCTTCTGCTTG-L
23	rAppTGTTATCGTATGCCGTCTTCTGCTTG-L
24	rAppTGCCATCGTATGCCGTCTTCTGCTTG-L

rApp indicates riboadenosine modification linked to the 5′-O group of the respective DNA oligonucleotide by a pyrophosphate group. -L refers to a 3′-amino-modifier blocking group (Integrated DNA Technologies, code /3AmMO/).

List of 5′-adapters (for RNA ligaion/cDNA library preparation).

Adapter	Sequence
5′	GUUCAGAGUUCUACAGUCCGACGAUC

List of Set1 calibrators (for miRNA quantification and normalization).

Adapter	Sequence
cali_01	pUCCACGACGUCUCAUGUAUUUC
cali_04	pGGGUACCAUACCGGUUGUCUUA
cali_17	pUCAUGAGUCCGUACCUUGAUUG
cali_18	pAUCAUUUACGAUUCGGAGCUGU
cali_20	pGAUAGUUCGGGAUCGCUGUAAC
cali_24	pUGCUACUCCGAUCUUUAGCCUC
cali_25	pAGGGCCCUUUAGGCACUAAUAG
cali_27	pGUAGCUGUCAGUACGUUCGUGC
cali_43	pUCUAGUUGCGUGAUGGAGAGAA
cali_44	pAGCCGCAUUUCGUAGUGAUAUU

List of Set2 calibrators (for miRNA quantification and normalization).

Adapter	Sequence
cali_07	pGUCCCACUCCGUAGAUCUGUUC
cali_11	pGAUGUAACGAGUUGGAAUGCAA
cali_12	pUAGCAUAUCGAGCCUGAGAACA
cali_14	pCAUCGGUCGAACUUAUGUGAAA
cali_15	pGAAGCACAUUCGCACAUCAUAU
cali_16	pUCUUAACCCGGACCAGAAACUA
cali_26	pAGGUUCCGGAUAAGUAAGAGCC
cali_28	pUAACUCCUUAAGCGAAUCUCGC
cali_31	pAAAGUAGCAUCCGAAAUACGGA
cali_35	pUGAUACGGAUGUUAUACGCAGC

List of RNA sequences used in ^{32}P–end-labeled ladder.

Length, nt	Sequence
19	CGUACGCGGGUUUAAACGA
24	CGUACGCGGAAUAGUUUAAACGUUUAAACUGU
30	CUUGGUCGUACGCGGAAUAGUUUAAACUGU
35	CUCAUCUUGGUCGUACGCGGAAUAGUUUAAACUGU
45	CUCAUCUUGGUCGUCUCGAUGGGUACGCGGAAUAG-UUUAAACUGU

^{32}P labeling of RNA and DNA ssRNA and ssDNA oligonucleotides. Ten picomoles of oligonucleotide were incubated with 1.7 pmol γ-^{32}P-ATP with a specific activity of 6,000 Ci/mmol and 10 U of T4 polynucleotide kinase (T4 PNK) (New England Biolabs) with 1× T4 PNK buffer in 10-μL reaction volume for 15 min at 37 °C. The reaction was quenched by addition of 10 μL of 50% formamide loading buffer, followed by 15% urea PAGE for 50 min at 30 W. The radiolabeled band, visualized by phosphorimaging of the gel, was excised and the labeled oligonucleotide was eluted overnight into 450 μL of 0.3 M NaCl. The supernatant was recovered from the gel slices, and oligonucleotide was precipitated by addition of 3.5 vol of absolute ethanol and incubation for 1 h on ice. The oligonucleotide pellet was collected by centrifugation at 13,000 × *g* for 30 min at 4 °C and dissolved in 10 μL of water.

Five hundred-nucleotide RNA transcript. One hundred nanograms of PCR product "RNAseq cal" was in vitro transcribed at 37 °C for 2 h in 1× T7 buffer with 4 mM GTP, 2.5 mM CTP, 1 mM UTP, and 2.5 mM ATP in a total volume of 50 μL using 60 pmol of α-^{32}P-UTP with a specific activity of 800 Ci/mmol, purified using a MicroSpin G-25 column (Illustra) and 4% urea PAGE. The labeled full-length product was visualized by phosphorimaging and then excised from the gel for elution in 400 μL of 0.3 M NaCl overnight, precipitated for 30 min on ice after addition of 3 vol of absolute ethanol, and collected as a pellet via centrifugation at 13,000 × *g* for 10 min at 4 °C. The supernatant was aspirated, and the pellet containing the radiolabeled transcript was air-dried for 5 min and reconstituted in 20 μL of water.

Double-stranded nucleotide dsDNA oligonucleotides. Purified 680-nt PCR amplicon (4 μg) based on the EIF4E coding sequence was digested at 37 °C for 2 h in a total volume of 400 μL using 100 U of MnlI restriction enzyme in 1× CutSmart buffer (New England Biolabs). Dephosphorylation was performed for 4 h at 37 °C in 600 μL of 1× Antarctic Phosphatase (AnP) Reaction Buffer and 100 U of AnP (New England Biolabs), followed by heat inactivation at 65 °C for 20 min. Cleavage products were precipitated by adding 3 vol of ethanol followed by incubation on ice for 30 min, and 30-min centrifugation at 13,000 × *g*. The supernatant was removed, pellet air-dried for 5 min and resuspended in 30 μL of water, subjected to gel filtration using Microspin-G25 columns (Illustra), then radiolabeled using 1× PNK buffer, 3 U of T4 PNK (New England Biolabs), and 5.0 pmol of γ-^{32}P-ATP with a specific activity of 6,000 Ci/mmol, followed by addition of 100 pmol of nonradioactive ATP. Products were separated by 15% urea PAGE 50 min at 30 W and purified as described for ssRNA/ssDNA oligonucleotides (see above).

Use of ^{32}P-labeled tracer mixes to optimize isolation from biofluids. Combinations of synthetic 5′-^{32}P–labeled spike-in ssRNA (19 nt, 24 nt, 21 nt 2′-*O*-meRNA, and 45 nt) and ssDNA (31 nt) oligonucleotides were used to monitor degradation resulting from ribonuclease activity during and after purification (see input lanes, Figs. 1 and 2). Less than 0.1 pmol per oligonucleotide were added to the initial denaturation condition of each sample. In conditions without an initial denaturation step, the tracer mixture was added with the organic extraction agent. Nucleic acids collected in water or 10 mM Tris after RNA and DNA isolation were separated on a 17.5% urea PAGE gel and visualized by phosphorimaging after overnight incubations and compared with the equivalent amount of input mixture used in the respective experiment.

Experiment A: Hot preincubation, organic extraction, and RNA precipitation. One hundred fifty microliters of water controls and serum samples were either directly extracted with 3 vol of TRIzol LS reagent (Thermo Fisher Scientific) (lanes 1 and 2) or mixed 1:1 with 50 °C-preheated denaturation solutions containing either 4% SDS, 4 mM EDTA, 20 mM Tris·HCl, pH 7.5 (lane 3), or 8 M GITC, 80 mM Na citrate, 0.13 g of sarcosyl, and 50 mM 2-mercaptoethanol (lane 4). Preheated samples were incubated at 50 °C for 5 min, cooled to room temperature for 2 min, followed by organic extraction with 3 vol of TRIzol LS (SDS-denatured samples) or acidic phenol (GITC-treated samples). Phase separation was induced in all conditions by addition of 0.2 vol of chloroform. After adding 1/10 vol of 3 M Na acetate, pH 4.6, the aqueous phases were reextracted with 1 vol of phenol/chloroform/isoamylalcohol (25:24:1) and precipitated with 3 vol of ethanol. Samples were incubated on ice for 30 min, spun at 12,000 × *g* for 30 min. Then supernatants were carefully removed and pellets were air-dried until glossy and resuspended in 20 μL of water.

Experiment B: Hot preincubation, organic extraction, and RNA column purification. Preincubation and extraction conditions were identical to experiment A. Phase separation in all samples was induced by addition of 0.2 vol of chloroform. After addition of 1/10 vol of 3 M Na acetate, pH 4.6, and 1.5 vol of ethanol, the aqueous supernatants were subjected to column purification using the RNeasy minElute cleanup protocol for serum/plasma using buffer RWP and RPE (Qiagen), following the instructions by the manufacturer. Samples were eluted from the columns in 20 μL of water. Column flowthrough fractions of aqueous phases were subjected to nucleic acid precipitation by adding additional

1.5 vol of ethanol, followed by cooling on ice for 30 min, centrifugation at 12,000 × *g* for 30 min, aspiration of the supernatant, and air drying of the pellets until they appeared glossy, followed by dissolving the pellets in 20 μL of water.

Experiment C. Experimental conditions are the default reaction conditions used for the serum and plasma (see below), using either manual extractions in Eppendorf tubes or automated extraction conditions in a 96-well 1-mL deep-well plate. Where indicated, proteinase K was left out during hot preincubation. Reaction tubes were photographed after inducing phase separation and centrifugation.

Experiment D. For detergent denaturation/proteinase K digestion, 250-μL serum samples were mixed 1:1 with 50 °C-preheated denaturation solutions containing either 4% SDS, 4 mM EDTA, 20 mM Tris·HCl, pH 7.5, or 8 M GITC, 80 mM Na citrate, 0.13 g of sarcosyl, 50 mM 2-mercaptoethanol, and incubated at 50 °C for 2 min. Fifty micrograms of proteinase K were added, and the solution was incubated for 15 min at 50 °C. After digestion, solutions were cooled to room temperature for 2 min, followed by organic extraction with 1.5 vol of 4 M GITC extraction solution or acidic phenol. Phase separation in all samples was induced by addition of 0.2 vol of chloroform. After addition of 1/10 vol of 3 M Na acetate, pH 4.6, and 1.5 mL of ethanol, the aqueous supernatants were subjected to column purification using the RNeasy minElute cleanup protocol for serum/plasma using buffer RWP and RPE (Qiagen), following the extraction conditions of the manufacturer, except for column binding and washing in the presence of 66% isopropanol. Samples were eluted from the columns in 20 μL of water.

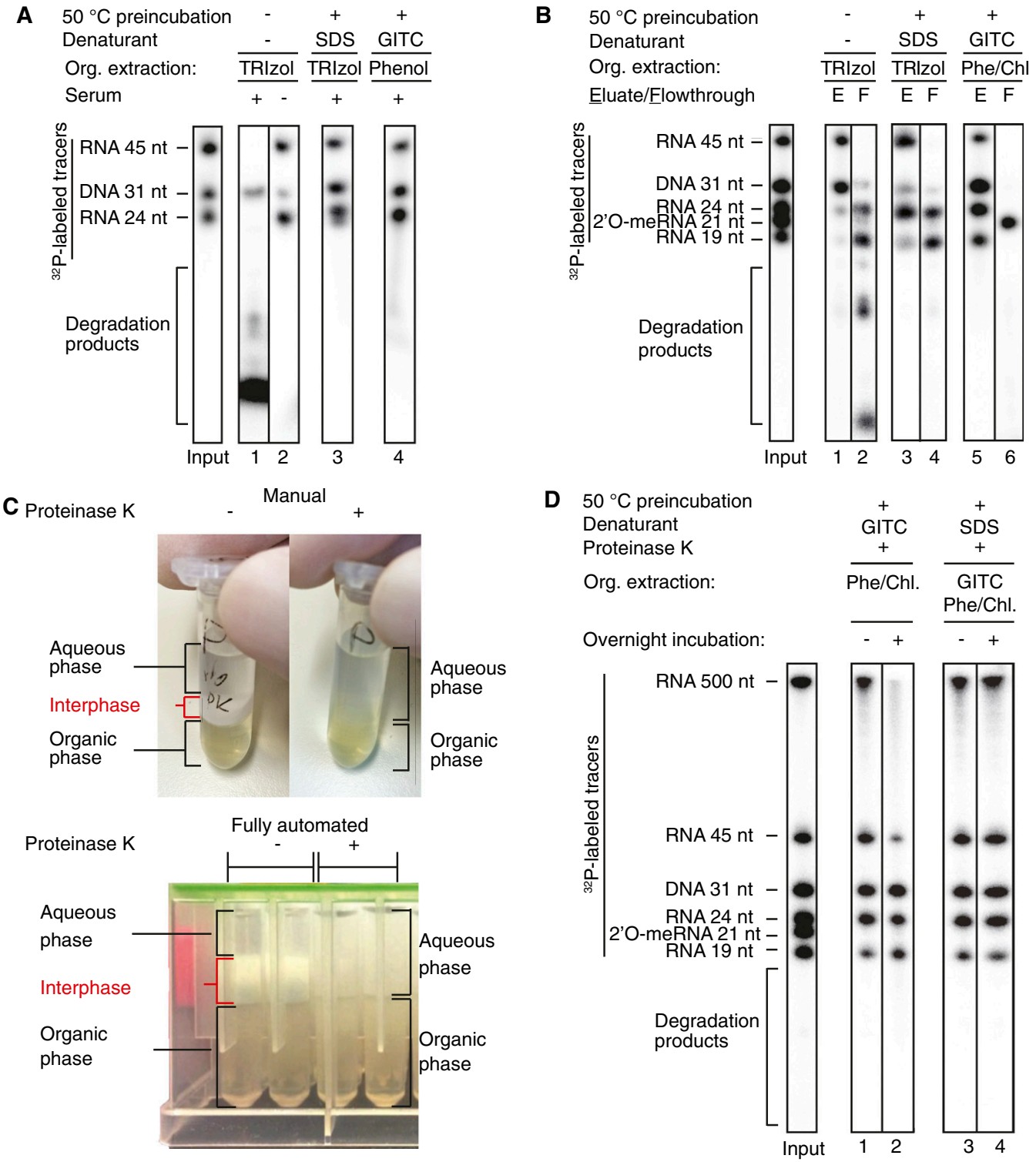

Fig. S1. Method optimization. (*A*) RNA degradation during RNA isolation is a consequence of residual RNase activity in the samples, which can be reduced by initial hot preincubation in denaturants. (*B*) Combining initial hot sample denaturation with column purification further reduces RNase activity and increases RNA intactness in exRNA isolation. (*C*) Initial hot denaturation and proteinase K digestion does eliminate interphase formation in extraction-based methods. (*D*) Interphase-deprived RNA extraction and column purification further improves RNA integrity.

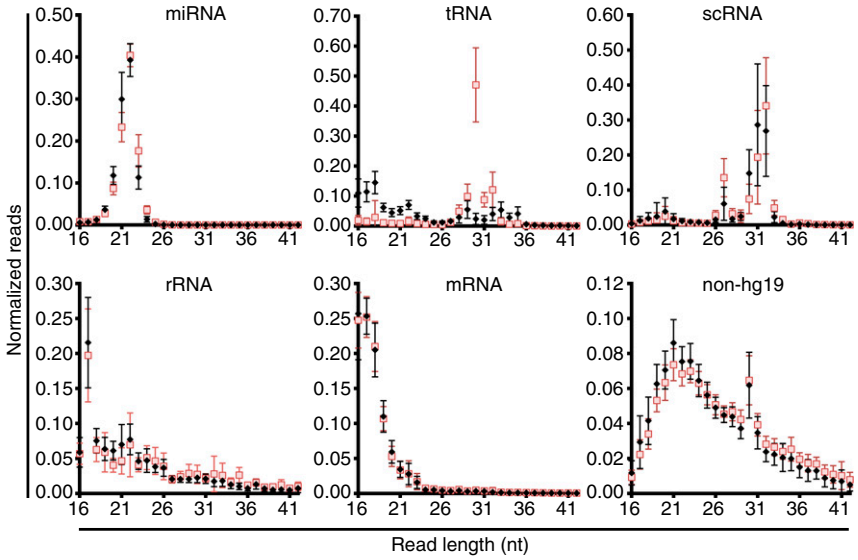

Fig. S2. Mean read length distributions of 5′P/3′OH-containing exRNAs in biofluids. EDTA plasma (black diamonds) and serum (red squares) featuring individual sRNA classes (miRNAs, tRNA, scRNAs, rRNAs), mRNA, and non-hg19 reads are shown. Error bars indicate SDs from the mean.

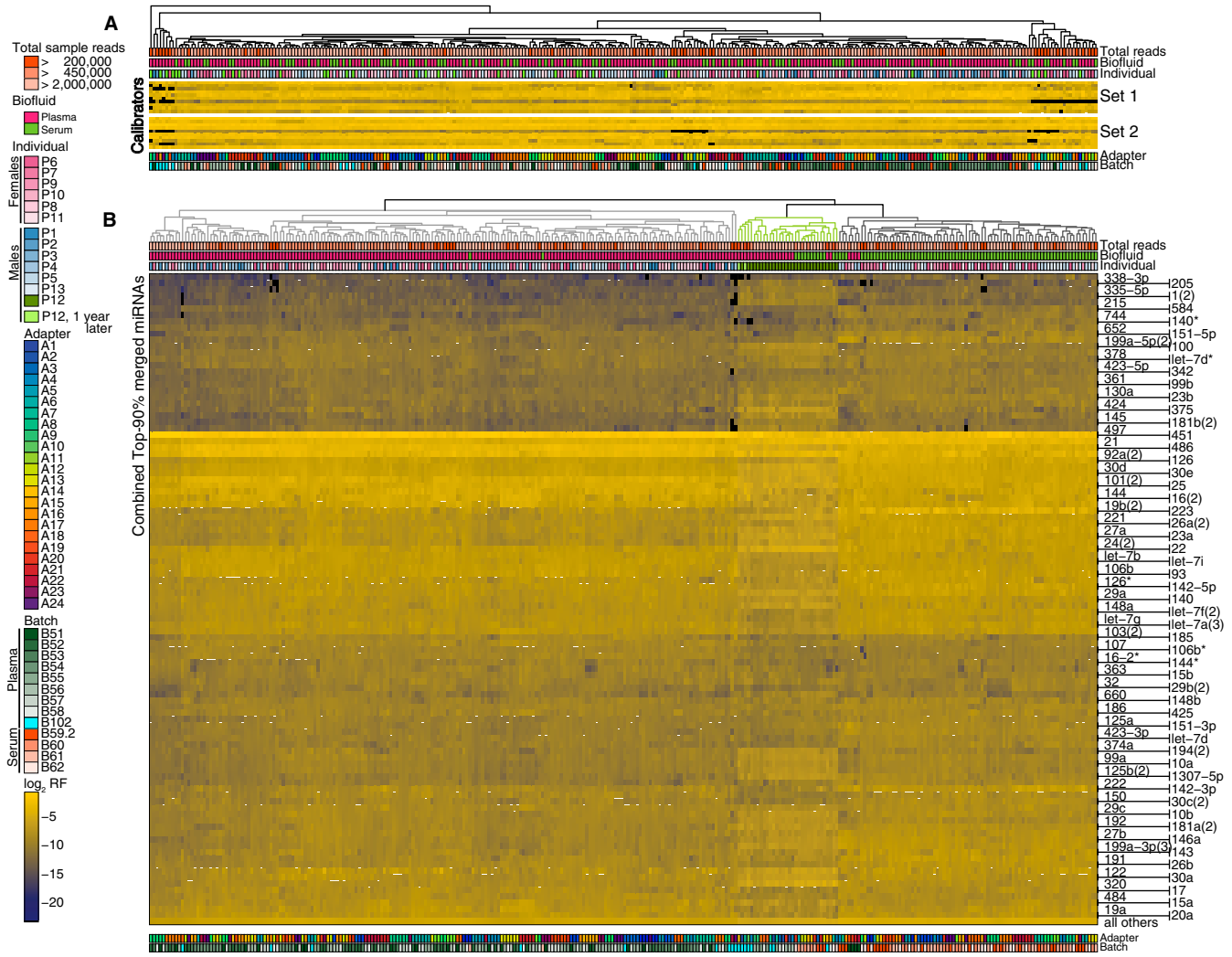

Fig. S3. Unsupervised clustering of miRNAs from human biofluid samples reveal distinct miRNA signatures for serum and plasma and uncovered a unique miRNA profile for subject P12. This figure features the same content and layout as Fig. 2 but includes samples with ≥100,000 hg19-mapped reads. (*A*) The calibrator heatmap reports unsupervised clustering of two sets of 10 synthetic 22-nt 5′P/3′OH-containing oligoribonucleotides spiked into samples at the beginning of RNA isolation (Set1) and before small RNA cDNA library preparation (Set2). (*B*) The miRNA heatmap is based on the union of the top 90% of miRNAs present in any sample. Sample order (columns) and miRNA arrangement (rows) were subjected to hierarchical clustering. All biofluid samples from study subject P12 (green) clustered together yet were different from the rest of samples.

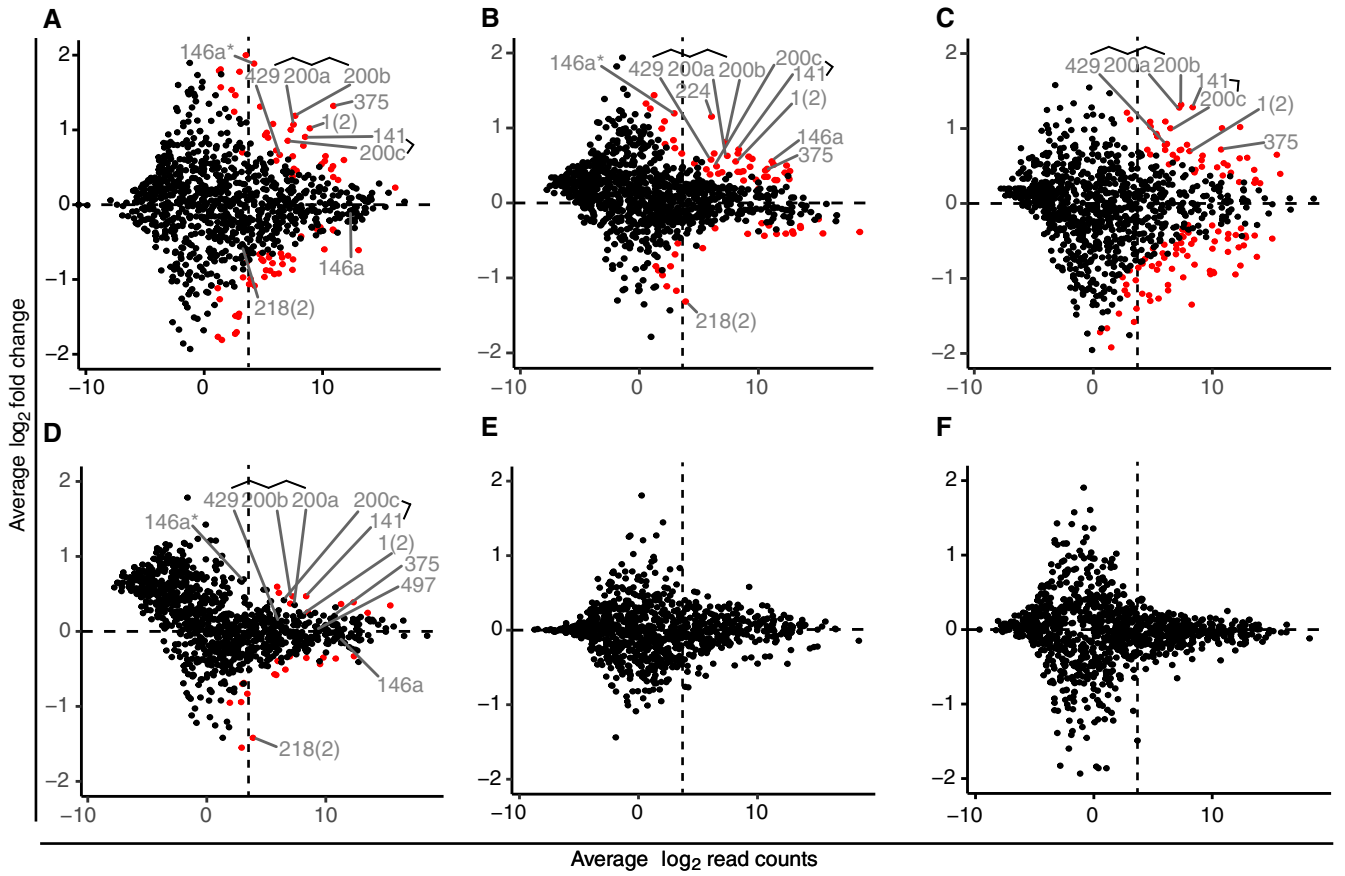

Fig. S4. Differences in miRNA abundance based on gender, female hormonal cycle, and prandial state. This figure was generated in accordance with Fig. 3 and features complementary content. Unless stated otherwise, read normalization was performed considering all miRNAs. Count data of subject P12 were excluded from all comparisons. (*A*–*C*) Effect of gender, (*A*) comparing female vs. male (serum) (for the corresponding plasma vs. plasma comparison, see Fig. 3*G*); (*B*) comparing female vs. male (plasma) but additionally excluding female subject P11. (*C*) Comparison of subject P11 to other female study subjects (plasma). (*D*) Comparison of two random groups consisting of three male and three female volunteers each (P1, P3, P5, P9, P10, and P14 vs. P2, P4, P6, P7, P11, and P13). (*E*) Effect of menstrual cycle, comparing follicular vs. luteal state (serum). For the corresponding plasma vs. plasma comparison, see Fig. 3*H*. (*F*) Effect of fasting: preprandial vs. 1-h postprandial state, plasma. For the corresponding 4-h preprandial vs. postprandial state comparison, see Fig. 3*I*.

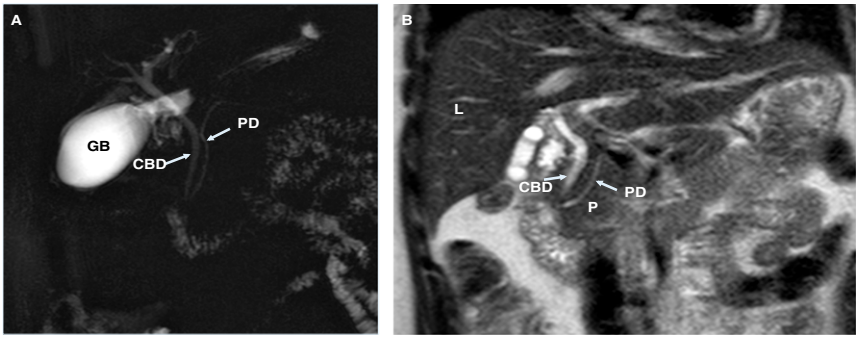

Fig. S5. MRI imaging of individual P12: (*A*) Thick-slab magnetic resonance cholangiopancreatography image showing normal biliary tree, common bile duct (CBD), pancreatic duct (PD), and gallbladder (GB). (*B*) Coronal T2-weighted MR image showing liver (L), pancreas (P), common bile duct (CBD), and pancreatic duct (PD). No abnormalities are revealed.

Table S1. Demographic and additional metadata data of study participants

Individual	Age, y	Sex, M/F	Race/ethnicity	BMI	Initial weight, lb	Height, in.	Smoker	Drugs of abuse	Sleep schedule, Di/N	Sleep pattern, R/D	Exercise, >3 h/wk	Blood draws	
												First	Last
P1	43	M	White	26.3	194	76.0	Y	N	Di	R	Y	11/19/14	1/5/15
P2	32	M	White	24.9	176	70.0	N	N	Di	R	N	11/20/14	1/21/15
P3	38	M	Hispanic	23.2	176	73.0	N	N	Di	R	Y	12/1/14	1/12/15
P4	25	M	Asian	22.0	149	69.0	N	N	Di	R	Y	12/1/14	1/12/15
P5	27	M	White	23.7	170	71.0	N	N	Di	R	N	12/15/14	1/26/15
P6	36	F	Biracial	22.7	163	71.0	N	N	Di	D	Y	1/6/15	2/17/15
P7	31	F	White	21.4	125	64.0	N	N	Di	R	N	1/26/15	3/9/15
P8	35	F	Biracial (Hispanic/ white)	22.2	140	66.5	N	N	Di	R	N	2/2/15	2/23/17
P9	41	F	Asian	24.9	150	65.0	NR	NR	Di	D	Y	2/2/15	3/18/15
P10	24	F	White	24.6	130	61.0	N	N	Di	R	N	2/9/15	3/23/15
P11	24	F	Asian	18.5	125	69.0	N	N	Di	R	Y	2/9/15	3/25/15
P12	26	M	White	24.4	175	71.0	N	N	Di	R	Y	2/11/15	3/25/15
P13	30	M	Hispanic	23.4	154	68.0	N	N	Di	R	Y	2/11/15	3/25/15

Abbreviations: BMI, body mass index; D, disturbed; Di, diurnal; F, female; M, male; N, nocturnal; NR, not recorded; R, regular.

Table S2. Statistical analysis of individual miRNA concentration ranges in plasma samples of healthy study participants

Plasma	P1	P2	P3	P4	P5	P6	P7	P8	P9	P10	P11	P12	P13
P1		—	—	—	—	—	—	—	—	—	—	<0.0001	—
P2			—	—	—	—	—	—	—	—	—	<0.0001	—
P3				—	—	—	—	—	—	—	—	<0.0001	—
P4					—	—	—	—	—	—	—	<0.0001	—
P5						—	—	—	—	—	0.0062	<0.0001	—
P6							—	—	—	—	—	<0.0001	—
P7								—	—	—	—	<0.0001	—
P8									—	—	0.0004	0.0002	—
P9										—	—	<0.0001	—
P10											—	<0.0001	—
P11												<0.0001	—
P12													<0.0001
P13													

Plasma sample miRNA concentrations based on Set1 calibrator reads, their molar amounts, and miRNA read counts were compared between individuals using the Tukey multiple-comparison test. Only comparisons of high significance ($P \leq 0.01$) were considered.

Table S3. Statistical analysis of individual miRNA concentration ranges in serum samples of healthy study participants

Serum	P5	P6	P8	P9	P12	P13
P5		—	—	—	<0.0001	—
P6			—	—	<0.0001	—
P8				0.0037	0.0002	—
P9					<0.0001	—
P12						<0.0001
P13						

Serum sample miRNA concentrations based on Set1 calibrator reads, their molar amounts, and miRNA read counts were compared between individuals, using the Tukey multiple-comparison test. Only comparisons of high significance ($P \leq 0.01$) were considered.

Table S4. Laboratory results of study subject P12

Test	Result	Reference range	Test	Result	Reference range
Mitochondria antibody	Negative	(Negative)	Hemoglobin A1C	5.4%	(4.7–6.4)%
Albumin	4.5 g/dL	(3.9–5.1) g/dL	Estimated average glucose	108 mg/dL	(88–137) mg/dL
Total bilirubin	0.6 mg/dL	(0.2–1.2) mg/dL	Ferritin	80 ng/mL	(25–270) ng/mL
Direct bilirubin	0.2 mg/dL	(0.1–0.3) mg/dL	White blood cell count	6.2 k/μL	(4.8–10.8) k/μL
Alk phos	78 U/L	(45–132) U/L	Red blood cell count	4.83 MIL/μL	(4.50–5.90) MIL/μL
Alanine transferase	14 U/L	(0–30) U/L	Hemoglobin	14.6 g/dL	(14.0–17.4) g/dL
AST	16 U/L	(13–50) U/L	Hematocrit	42.2%	(41.5–50.1)%
Total protein	7.2 g/dL	(6.0–8.5) g/dL	Mean corpuscular volume	87.4 fL	(80.0–96.0) fL
Anti smooth muscle Ab	Negative	(Negative)	Mean corpuscular hemoglobin	30.2 pg	(27.0–33.0) pg
Hep B surf Ab qual	Positive	(Negative)	Mean corpuscular hgb concen	34.6 g/dL	(33.0–36.0) g/dL
Hep B surface Ag	Nonreactive	(Nonreactive)	Red cell distribution list	12.0%	(11.9–15.3)%
Hep C Ab	Nonreactive	(Nonreactive)	Platelet count	245 k/μL	(150–400) k/μL
Lipase	78 U/L	(10–195) U/L	Mean platelet volume	11.0 fL	(8.0–12.0) fL
Amylase	78 U/L	(18–100) U/L	nRBC	0.00 k/μL	
Thyroid stimulating hormone	1.85 μU/mL	(0.400–4.60) μU/mL	Nucleated RBCs	0.0/100 WBC	
Free thyroxine Ft4	1.29 ng/dL	(0.80–1.70) ng/dL	Neutrophil %	55%	
Urine color	Yellow	(Yellow)	Neutrophils (Auto Diff#)	3.4 k/μL	(1.8–7.7) k/μL
Appearance, urine	Clear	(Clear)	Lymphocytes (Auto Diff%)	35%	
Urine specific gravity	1.019	(1.006–1.029)	Lymphocytes (Auto Diff#)	2.2 k/μL	(1.0–4.8) k/μL
Urine pH	6.5 pH	(5.0–8.0) pH	Monocytes (Auto Diff%)	7%	
Protein urine random	Negative mg/dL	(Negative) mg/dL	Monocytes (Auto Diff#)	0.5 k/μL	(0.3–0.5) k/μL
Urine glucose	Negative mg/dL	(Negative) mg/dL	Eosinophil %	2%	
Ketone, urine	Negative mg/dL	(Negative) mg/dL	Eosinophils (Auto Diff#)	0.1 k/μL	(0.1–0.3) k/μL
Blood urine	Negative	(Negative)	Basophil %	1%	
Urine urobilinogen	0.2 EU/dL	(0.1–1.0) EU/dL	Basophils (Auto Diff#)	0.04 k/μL	(0.00–0.05) k/μL
Urine nitrites	Negative	(Negative)	Immature granulocyte count	0.01 k/μL	(0.00–0.07) k/μL
Urine leukocytes	Negative	(Negative)	Sodium	143 mEq/L	(135–145) mEq/L
Urine bilirubin	Negative	(Negative)	Potassium	4.4 mEq/L	(3.5–5.0) mEq/L
Vitamin B12	609 pg/mL	(211–946) pg/mL	Chloride	103 mEq/L	(98–108) mEq/L
Vitamin D 25-hydroxy total	30.3 ng/mL	(>30.0) ng/mL	Carbon dioxide	25 mEq/L	(22–29) mEq/L
Albumin	4.6 g/dL	(3.9–5.1) g/dL	Blood urea nitrogen	13 mg/dL	(5–21) mg/dL
Total bilirubin	0.5 mg/dL	(0.2–1.2) mg/dL	Creatinine	1.10 mg/dL	(0.50–1.50) mg/dL
Direct bilirubin	0.2 mg/dL	(0.1–0.3) mg/dL	GFR MDRD non-AF Amer	>60 mL/min/BSA	(>60) mL/min/BSA
Alk phos	93 U/L	(45–132) U/L	Glucose	76 mg/dL	(70–115) mg/dL
Alanine transferase	13 U/L	(0–30) U/L	Calcium	9.6 mg/dL	(8.5–10.5) mg/dL
AST	17 U/L	(13–50) U/L	Anion gap	15 mEq/L	(7–16) mEq/L
Total protein	7.5 g/dL	(6.0–8.5) g/dL			
Cholesterol	136 mg/dL	(133–200) mg/dL			
Triglycerides	177 mg/dL	(46–150) mg/dL			
HDL cholesterol	48 mg/dL	(40–60) mg/dL			
LDL cholesterol direct	53 mg/dL	(0–130) mg/dL			
Chol/HDL	2.8 ratio	(0.0–5.0) ratio			

Complete blood count, comprehensive metabolic testing, liver function testing, and lipid profiles were within normal ranges.

Dataset S1. Per-sample metadata and exRNA read statistics

Dataset S1

Metadata annotations from the patient evaluation sheet are listed in columns B to U, additional metadata categories optimized for scripted data processing in unsupervised clustering and differential expression analyses are listed in columns AI to AX. Per-sample read statistic are detailed in columns V to AH.

Dataset S2. Per-sample merged miRNA read frequencies and metadata annotations used for unsupervised clustering

Dataset S2

Metadata categories are detailed in rows 1–17, read frequencies of merged miRNAs as reported by the in-house RSDAP (40) are listed in rows 18–1,534, and sample data are tabulated from column A to LA.

Dataset S3. Per-sample merged miRNA read counts and metadata annotations used for differential expression analyses

Dataset S3

Metadata categories are detailed in rows 1–17, and read counts of merged miRNAs as reported by the in-house RSDAP (40) are listed in rows 18–1,534. Sample data are tabulated from columns A to LA.

Dataset S4. Differences in miRNA abundance based on type of biofluid, individual P12, gender, female hormonal cycle, and prandial state

Dataset S4

DESeq2-based DEA tables in sheets list miRNA abundance changes and were used to generate MA plots in Fig. 3. Each table lists base mean abundances (baseMean), lfcs (log2FoldChange), $\log_2$ fold change SEs (lfcSE), Wald statistics (stat), Wald test *P* values (pvalue), and Benjamini and Hochberg adjusted *P* values (p_{adj}). lfcs were computed based on merged miRNA read counts utilizing all detectable miRNAs across all samples for SFE/normalization, unless stated otherwise. DEA analyses utilizing Set1 calibrator or miR-451 and 144 read counts for SFE were provided in addition to default computations for serum to plasma comparisons (A) and for P12 vs. other male comparisons (B1 and B2) on additional sheets; their names were extended "_set1" and "_451,144," accordingly, and another sheet with name extension "_comparison" was added. All tables display lfcs with a base mean abundance of at least 10 normalized reads, and lfcs with a significance level of $P_{adj} \leq 0.05$; if miRNAs with lesser mean abundance or comparisons of lesser significance are of interest, these margins can be adjusted in the respective data table Excel files. (A) Serum vs. plasma, excluding individual P12. (B1 and B2) Study subject P12 vs. all other individuals comparing miRNA abundances for plasma and serum, respectively. (C1–C4) Effect of gender. Excluding individual P12, in plasma (C1) and serum (C2), respectively; (C3) like C1, but additionally excluding female P11, who showed higher epithelial miRNA contributions than other female study subjects, which are detailed in a comparison of individual P11 to other females (C4). (C5) Comparison of two random subsets featuring three male and female study participants. (D1 and D2) Effect of menstrual cycle comparing follicular and luteal phases, in plasma (D1) and serum (D2), respectively. (E1–E4) Effect of fasting: miRNA abundance in plasma, comparing preprandial vs. postprandial state at 1 h (E1), and preprandial vs. postprandial state at 4 h (E2). miRNA abundance in serum, comparing preprandial vs. postprandial state at 1 h (E3), and preprandial vs. postprandial state at 4 h (E4).

Other Supporting Information Files

SI Appendix (PDF)